INDEX COPERNICUS
INTERNATIONAL



Bio-Algorithms and Med-Systems

WWW.BAMSJOURNAL.COM ISSN: 1896-530X

ORIGINAL ARTICLE

Received: 29.07.2024
Accepted: 26.10.2024
Published: 11.12.2024

CITE THIS ARTICLE AS:
Lang K, "Image-Guided FLASH Proton Therapy. A dream? Naivety? Arrogance? Or a Necessity?," Bio-Algorithms and Med-Systems vol. 20, special issue, pp. 17-26, 2024, DOI: 10.5604/01.3001.0054.8930

AUTHORS' CONTRIBUTION:
A. Conceptualization
B. Data Curation
C. Formal Analysis
D. Funding Acquisition
E. Investigation
F. Methodology
G. Project Administration
H. Resources
I. Software
J. Supervision
K. Validation
L. Visualization
M. Writing – Original Draft
N. Writing – Review & Editing

CORRESPONDING AUTHOR:
Karol Lang; The University of Texas at Austin, Austin, Texas, USA; E-mail: lang@physics.utexas.edu

COPYRIGHT:
Some rights reserved: Jagiellonian University Medical College. Published by Index Copernicus Sp. z o. o.

OPEN ACCESS:
The content of the journal „Bio-Algorithms and Med-Systems" is circulated on the basis of the Open Access which means free and limitless access to scientific data.

CREATIVE COMMONS CC BY:
Attribution. It is free to copy, distribute, present and perform the copyrighted work and derivative works developed from it, provided that the name of the original author is cited.

Image-Guided FLASH Proton Therapy. A dream? Naivety? Arrogance? Or a Necessity?

Karol Lang[1]
[1]The University of Texas at Austin, Austin, Texas, USA

ABSTRACT

Objective: The in-vivo therapy guidance by imaging and dosimetry of proton irradiations, generically known as proton range verification, are some of the most underinvested aspects of radiation oncology. They trail behind other advances in radiation therapy due to the scarcity of sensitive instruments compounded by the lack of treatment protocols for precision monitoring of effects of beam radiation. This is despite that such measurements may dramatically enhance the treatment accuracy and lower the post-radiation toxicity, thus improving the entire outcome of cancer therapy.
Methods: In this contribution, we focus on the motivation of designing and building of an in-beam time-of-flight (ToF) positron-emission-tomography (PET) scanner with the depth--of-interaction (DoI) capability for high sensitivity and improved fidelity of imaging. A scanner could be augmented with a tungsten collimator that would enable prompt-gamma imaging (PGI) via single-photon emission computed tomography (SPECT) technique.
Results: We present selected results of our pre-clinical experiments with a FLASH proton beam and discuss other related ideas towards improving and expanding the use of PET/PGI/SPECT detectors for proton therapy. A scanner provides an access to data during the spill and past the spill permitting to capture the beam interaction and kinetic monitoring of its effect thus allowing a thorough assessment of each irradiation.
Conclusions: A novel scanner for multiple modalities can substantially improve the treatment precision of proton therapy leading to less toxic outcome of irradiations. Using it in the FLASH modality would additionally expand the patient reach of proton therapy.

KEYWORDS

proton therapy, FLASH effect, image-guidance, proton range verification, brain cancer, PET scanner, nuclear medical imaging, radio-pharmaceuticals, theranostics, multi-modal treatment, AI/ML PET, CASTOR, TPPT Consortium

LIST OF ABBREVIATIONS

AI – artificial intelligence
CASToR – Customizable and Advanced Software for Tomographic Reconstruction
CT – computed tomography
CTR – coincidence time resolution
FLASH – ultra-high rate of high dose radiation
HDPE – High-Density Polyethylene
LOR – lines of response
LYSO – lutetium-yttrium oxyorthosilicate
ML – machine-learning
MRI – magnetic resonance imaging
PES – positron-emitting species
PET – positron-emission-tomography
PGI – prompt gamma imaging
PMMA – polymethyl metacrylate
ROS – reactive oxygen species
SPECT – single-photon emission computed tomography
TPPT – Time-of-Flight PET for Proton Therapy

FOUNDATIONS

The Context ("The Big Picture")

Medicine confronts two sobering oncological facts: (1) In 2022, there were an estimated 20 million new cancer cases worldwide [1]; and (2) about 50% of all cancer patients undergo radiation therapy. It is natural to pose a simple question: Can radiation treatment be applied better than it has been so far?

The term "better" is vague until we define it, so, for context, we recall that the pillars of cancer treatment also include surgery, cytotoxic chemotherapy, molecularly targeted therapy and immunotherapy. In our question, better radiotherapy refers to such goals as minimizing or avoiding post-radiation complications (toxicity), treating more patients with proton beam rather than gamma beam or lowering the cost of therapy. The list is longer and touches both technical and sociomedical issues, such as improved diagnostic instruments, better-specialized pharmaceuticals, cheaper and better radiological beams or enhanced imaging and dosimetry. Most of this can be further empowered by progress in artificial intelligence (AI) and machine-learning (ML) algorithms, which could permit new, modern theragnostic protocols. Here, we narrow our focus to possible image-guided FLASH proton therapy.

A huge majority of radiation treatments use gamma beams that can be accurately aimed but are sometimes compared to "carpet bombing" of a body due to their broad, unstoppable coverage that also affects healthy tissues and leads to unavoidable post-radiation toxicity. In many, perhaps most cases, radiation therapy may be dramatically improved by using a proton beam, which assures a well-delineated zone of energy deposition [2]. Additionally, such treatments could be accompanied by precise monitoring of the result of each therapeutic radiation session (i.e., fraction).

However, the access to proton therapy is limited. Even though the 122 proton treatment centers that currently exists around the world are projected to double in number over the next decade or so, despite high costs of building and operating such facilities, proton therapy will need an even further growth. The first dedicated hospital-based clinical facility started in Loma Linda in 1990. Merely 350,000 patients have been treated worldwide with protons so far, as illustrated in Fig. 1. It is critical that proton therapy becomes more accessible as an essential component of the *precision personal medicine* that is currently beginning to shape many aspects of modern medicine. It is not only natural but mandatory that this rapid growth of proton therapy be accompanied by improved accuracy, control, and verification of each irradiation.

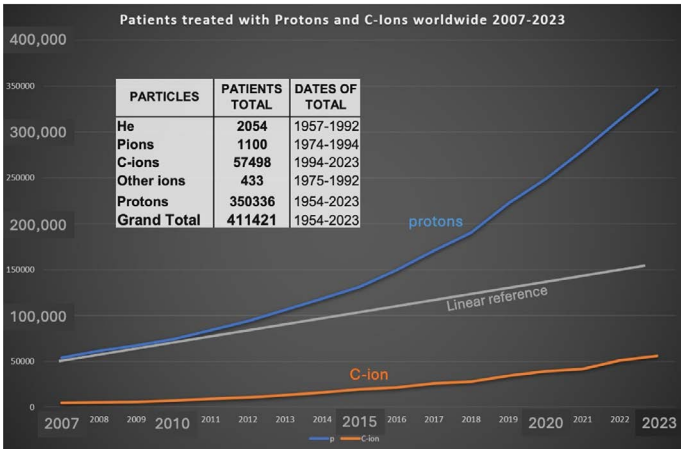

Fig. 1. Yearly numbers of patients treated in particle therapy facilities worldwide. Adapted from [3].

In-vivo Proton Range Verification

Much patient data derived from PET, CT and MRI scans are inputted for calculations of in-body beam interactions. Sophisticated anthropic modeling of radiation doses are nowadays a canonical part of comprehensive radiation treatment planning. However, much less feedback data are being acquired during the treatment itself. In most proton treatment centers, patients are only occasionally monitored by locally available imaging such as CT, Cone Beam CT or MRI, which are primarily sensitive to anatomical changes due to radiation, and PET scans, which could much better assess the state of cancer tissues and are primarily conducted after treatment.

Radiation treatments could be improved by mapping the delivery of beam energy (a.k.a. proton range verification). The in-vivo imaging and dosimetry of proton beams is (perhaps arguably) one of the most underinvested aspects of radiation cancer treatment, despite that such guidance and adaptive protocols could dramatically

improve the therapy outcome. The scarcity of sensitive instruments and absence of treatment protocols for precision monitoring of effects of beam radiation leaves much room for improvement. This is also despite that the tissue activation by the proton beam (Tab. I.) provides a "free" source of radiation, including positron-emitting species (PES), that could be used for imaging and dosimetry of each irradiation. This has been proposed in the past [4–16], we simply re-argue the case in the context of improved technology and beam deliveries.

Tab. I. The most common PET emitters activated in a human body via nuclear fragmentation processes during a proton therapy.

NUCLIDE ${}^{A}_{Z}X$	$T_{1/2}$ (min)	END-POINT (MeV)	NUCLEAR FRAGMENTATION PROCESSES *A(p, X)B*
${}^{10}_{6}C$	0.32	3.648	${}^{16}O(p, X){}^{10}C$ ${}^{14}N(p, X){}^{10}C$
${}^{11}_{6}C$	20.4	0.960	${}^{12}C(p, X){}^{11}C$ ${}^{13}C(p, X){}^{11}C$
${}^{13}_{7}N$	10.0	1.200	${}^{16}O(p, X){}^{11}C$ ${}^{14}N(p, X){}^{11}C$
${}^{15}_{8}O$	2.0	1.735	${}^{14}N(p, X){}^{13}N$ ${}^{16}O(p, X){}^{13}N$ ${}^{16}O(p, X){}^{15}O$

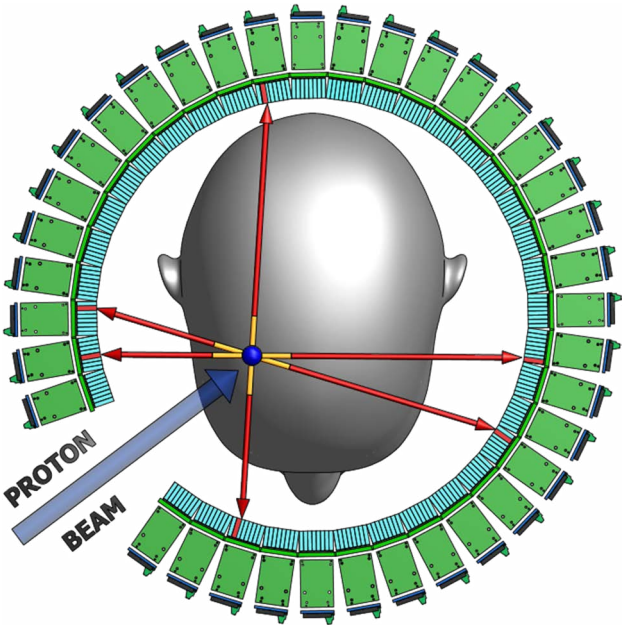

Fig. 2. A conceptual brain PET scanner for proton beam activation.

Determination of the in-vivo and *in-situ* effects of *each proton irradiation* remains challenging and requires the advancement of high-quality and high-sensitivity imaging and dosimetry. PET scanners [4–16] are the natural instruments of choice. As shown in Tab. I., the half-lives of the most abundant isotopes decaying via the β+ range from about 20 s for ${}^{10}_{6}C$, 2 min for ${}^{15}_{8}O$, to 20 min for ${}^{11}_{6}C$, thus necessitating an in-beam scanner (i.e., a scanner that can record positron emissions either concurrently with the therapeutic beam or immediately after irradiation). We illustrate such a brain PET scanner conceptually in Fig. 2. It would be a sensitive probe of both beam-activated PES and injected radiopharmaceuticals with positron-emitting isotopes. There are ideas as to how one can also consider additional imaging-enhancing pharmaceuticals [17].

Despite a byproduct of a therapeutic proton beam being the activation of elements in its path through a body, current therapeutic practice lacks protocols that exploit this diagnostic opportunity. It would require specialized scanners that are currently not available on the market. So tumors are rarely directly imaged or monitored during therapy. Novel instruments are needed to augment (i.e., modify) the accepted and the insurance-approved treatment protocols. This is a disruptive process but would lead to a better overall therapy outcome.

The FLASH Effect

In a conventional proton treatment, a typical patient receives 30 beam irradiations (fractions), each with a dose of 2 Gy, delivered over a period of up to a few minutes (for a total dose of 60 Gy). Recent observations with small animals point to a surprising and unexpected result known as the FLASH effect. It is achieved if the entire 60 Gy dose is administered in a much shorter time period of about a 1/10 of a fraction of a second. Studies suggest [18–31] that cancer tissues are eradicated as effectively as with a conventional beam, but, surprisingly and unexpectedly, the irradiated healthy tissues should tolerate 1,000 times higher intensity exposure. This effect is presently not understood and profoundly puzzles researchers [32–38]!

This discovery (or perhaps a rediscovery [39]) leads to unescapable conclusions, that (1) our understanding of the beam effects on live tissues is incomplete, and that (2) a large fraction (perhaps all) patients could receive better treatment. It is quite remarkable that despite radiation treatment being used for decades, the underlying fundamental time-dependent mechanism of how ionizing radiation interacts in live tissues is not fully grasped. This is currently the hottest issue debated in radiation oncology. Unfortunately, new relevant results on molecular dynamics emerge slowly, so any new data are precious for the discovery process.

Broadly suspected reactions that are responsible for the FLASH effect involve oxygen radicals, commonly known as reactive oxygen species (ROS) [32–38]. They help to destroy cancer tissues or impede the growth of cancer, but how does their time-dependent concentration alter their sparing of healthy tissue? More beam data taken with "intelligent" biochemical phantoms could help to illuminate this FLASH mystery.

Adaptive FLASH Protocols

We envision a clinical use of PET with FLASH beams. Such a treatment seems more promising than a conventional therapy, although it demands an even higher accuracy of beam delivery and more precise monitoring of its effects. Refining irradiation feedback will benefit from improved AI and ML software for reconstruction

and data processing that would both speed up and enhance the quality of imaging and dosimetry.

FLASH offers unique opportunities for PET imaging, since the time of activation is almost instantaneous. In a single FLASH "shot" (possibly a few FLASH fractions), the activation is compressed in time, resulting in the larger initial detection statistics and improved signal-to-noise ratio. This is in contrast with the higher-yield prompt-gammas that usually saturate current generation detectors. To our knowledge, the use of in-beam PET scanners for imaging and dosimetry of FLASH proton treatment has not been attempted, despite that such measurements and offer distinctive immediate assessment of irradiation and can be used for guiding the follow-on treatment. An adaptive FLASH therapy may not only improve the therapy outcome of individual patients, but is likely to increase the patient throughput and thus may extend such treatment to a much broader population.

However, before such novel protocols can find their clinical employment, the FLASH effect enigma must be resolved. Further understanding of in-vivo proton beam response, elucidation of the FLASH effect and clinical acceptance of FLASH extractions are all necessary. We stress that the effect of the better sparing of healthy tissue while efficiently eradicating cancer may revolutionize radiation oncology by improving outcomes and enabling much broader use of proton radiation treatment, which includes higher patient throughput. A "win-win" progress is feasible.

In-beam PET Scanners

There is an emerging consensus that sensitive and precise in--vivo PET imaging and dosimetry, the "holy grail" of irradiation diagnostics, should be introduced into treatment protocols to provide the necessary *feedback data that can adaptively guide the treatment and help assess irradiations results*. It would minimize short- and long-term post-radiation complications and lead to an improved overall therapy outcome. It requires an optimized arrangement between a beam and a high-resolution, high efficiency PET detector. Such protocols are likely essential for FLASH beam therapy, where an individual beam extraction is associated with large gradients of energy deposition. In-beam monitoring using PET scanners could provide the necessary real-time assessment of each irradiation, minimizing post-radiation toxicity and side-effects.

TPPT SCANNER

We have formed a consortium of researchers from Texas and Portugal [40] to build a high performance PET scanner and conduct preclinical tests at the Proton Therapy Center of the MD Anderson Cancer Center in Houston, Texas [41]. This Time-of-Flight PET for Proton Therapy (TPPT) Consortium has now designed, fabricated and commissioned an original PET brain scanner, shown in Fig. 3., for a fast, near real-time, response data analysis that addresses these *unmet needs* of oncology practiced in proton treatment centers.

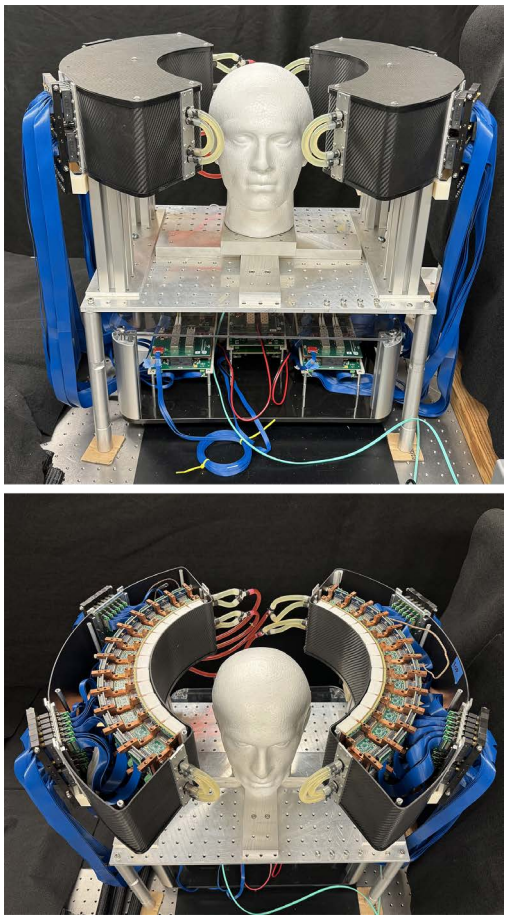

Fig. 3. Pictures of the TPPT brain PET scanner for use with proton beams in the Proton Therapy Center at the MD Anderson Cancer Center. The left photograph shows the inner instrumentation constructed out of LYSO crystal arrays (wrapped in white Teflon tape) and attached front-end electronics mounted on a SiPM of each crystal array. The copper "ribs" provide the over structural support, and the visible tubing is a part of the water cooling system needed for ASICs. The right photograph shows a fully assembled system.

Before conducting a suite of beam tests with phantoms at MD Anderson, we thoroughly characterized the scanner using a sealed stationary and moving ^{68}Ge linear source with an active volume of 1.4 mm in diameter and 16 cm in length [42, 43]. The tests resulted in adjusting the electronics for uniform gains, time alignment and yielded normalization factors of 6,144 LYSO crystals of dimensions 3 × 3 × 15 mm^3. These calibration procedures required that all 3,072 × 3,072 = 9,437,184 lines of response (LOR) were reconstructed and used in calculations.

Fig. 4. shows some performance parameters of our TPPT scanner derived from various calibration runs. We note the high performance level of our scanner, a result of the high-quality front-end electronics and data acquisition system [44] that reads SiPM Hamamatsu photodetectors [45]. These clean calibration data lead to very good energy resolution and coincidence time resolution (CTR) that for many LORs achieves less than 200 ps mark – better than in most commercial scanners.

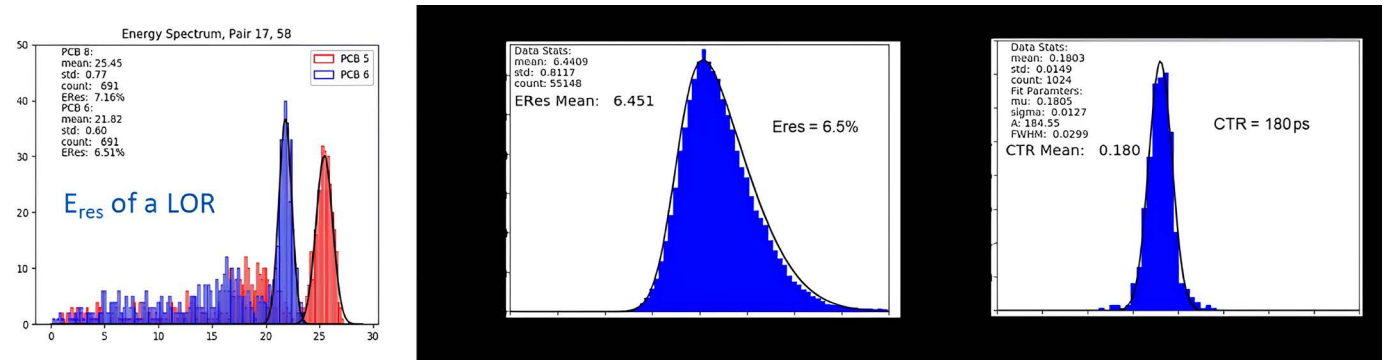

Fig. 4. Performance parameters of our TPPT brain PET scanner. Left: The energy spectrum with clearly visible photo peaks for one LORs identified by two crystal numbers. Center: The distribution of energy resolutions of all LORs. Right: The coincidence time resolution (CTR) of the most populated LORs.

FLASH TESTS

In parallel with our work on developing and testing the TPPT brain PET scanner, we have conducted tests with the ocular beam at MD Anderson, which has FLASH extraction capability. We constructed a setup that used only two spare 128-crystal modules that viewed a phantom irradiated by this beam, as illustrated in Fig. 5. Comprehensive summaries of our measurements were published earlier [46, 47], so here we present selected highlights in an abbreviated form.

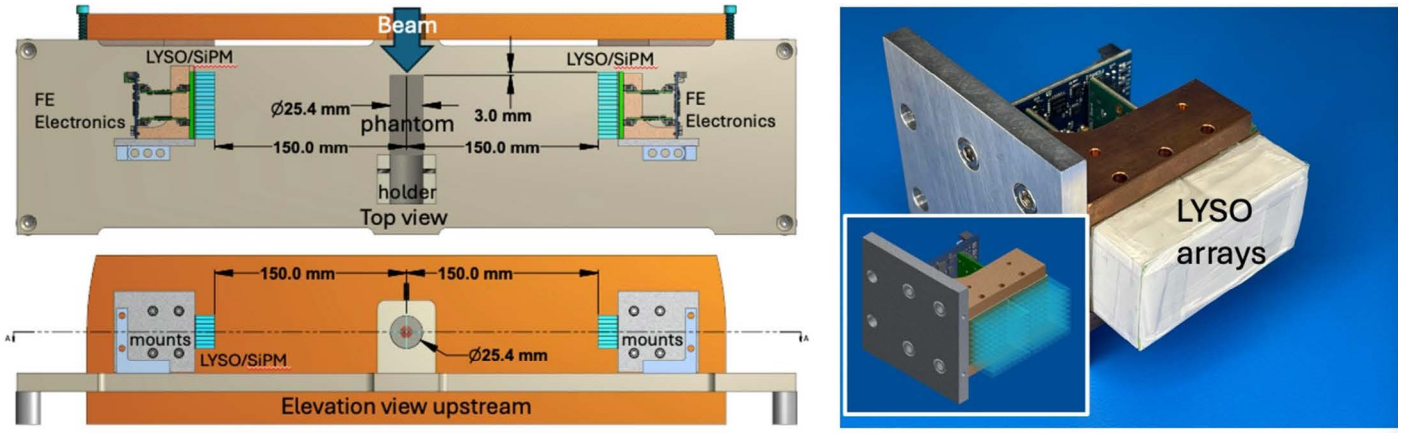

Fig. 5. Schematic top and elevation views (looking upstream), respectively, of a complete ocular beam setup at one of the exposure configurations. The beam direction is indicated by an arrow. PET modules are 2 × 64 scintillating LYSO crystal arrays, as shown on the right. They were read out by the front-end electronics provided by PETsys Electronics [44]. Figures borrowed from [47].

The FLASH beam had a 3.5×10^{10} proton with kinetic energy of 75.8 MeV, delivered in 101.5 ms long spills, yielding a dose rate of 164 Gy/s (further beam details can be found in [48]). We irradiated several phantoms and collected data for up to 20 min. Fig. 6. shows in-spill and post-spill coincidence rates between the two LYSO modules. In-spill coincidences are due to random hits due by prompt gammas. Post-spill coincidences are due to positron--emitting isotopes. We deduced this from the energy spectra plotted separately for in-spill and post-spill PET coincidence events, shown in Fig. 7. These are unprecedented tomography data that were captured in a FLASH beam for the first time.

For each FLASH "shot" the time-dependences of the post-spill coincidence rate was fit to an exponential function applying half-lives of expected dominant isotopes. These fits were then used to assess the relative abundance of each isotope. This procedure is shown in Fig. 8. Our measurements are sensitive to the depth of beam penetration into the phantom (i.e., the depth at which isotopes were produced). This reflects the sensitivity to energy--dependent activation cross sections as the beam ranges out. We also note that a high-sensitivity scanner (tightly surrounding the brain) can reconstruct 3-gamma images and measure the lifetime of positronium, which could provide an additional marker related to the density of tissues struck by a proton beam [49].

Our FLASH data analysis also included dosimetry and imaging of positron emissions. Fig. 9. and 10. show some results of this work. We employed the CASToR imaging package [50] to reconstruct

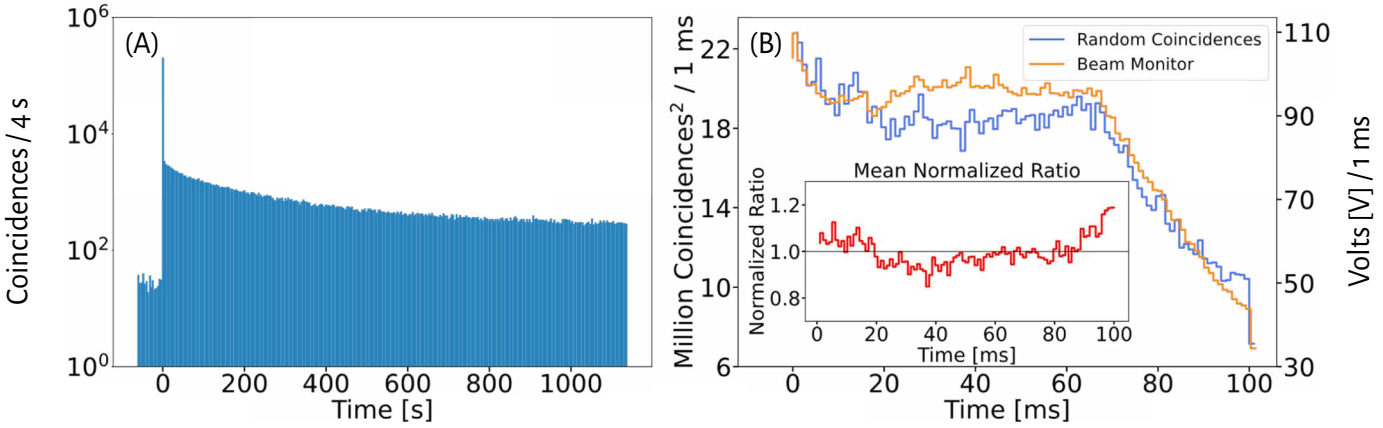

Fig. 6. (A) The number of PET coincidences as a function of time during a 20-minute data acquisition period with a water phantom. PET modules were placed 210 mm from the beam's center. The spill occurred at the 62 sec mark. The activity before the spill is due to prior spills; (B) A comparison between PET random single coincidences to the beam monitor output voltage per 1 ms. The mean normalized ratio between the two quantities as a function of time is displayed in the inset. Figures borrowed from [47].

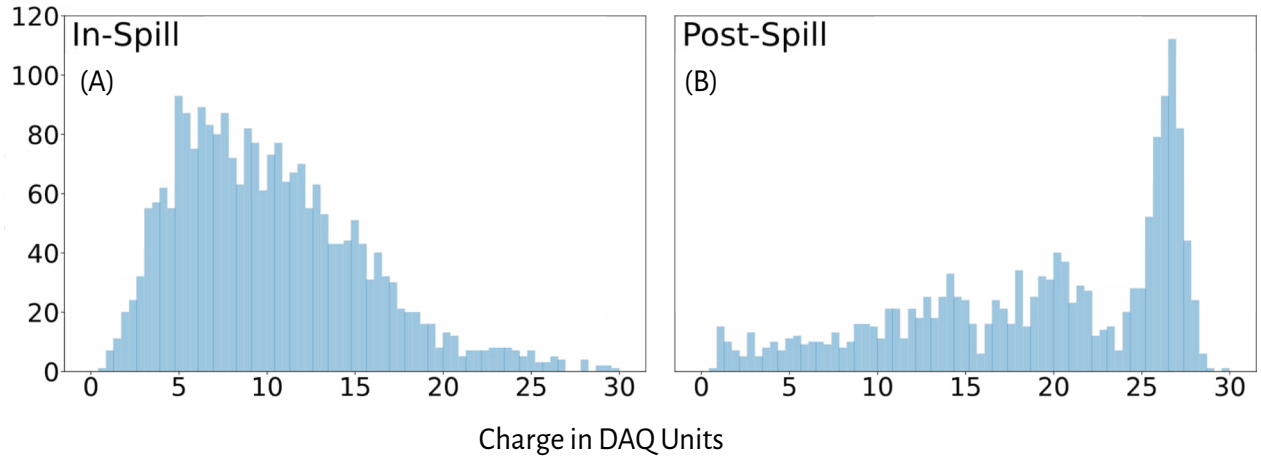

Fig. 7. (A) An energy spectrum acquired in a single pixel crystal *during* the 101.5 ms beam spill irradiating a water phantom, and (B) an energy spectrum for events after the beam spill. The photopeak at DAQ units of about 27 is due to 511 keV gammas. The absence of photopeak in the energy spectrum during the beam spill (the "in-spill" data) evinces that the radiation environment during the beam spill is dominated by prompt gammas. Figures borrowed from [47].

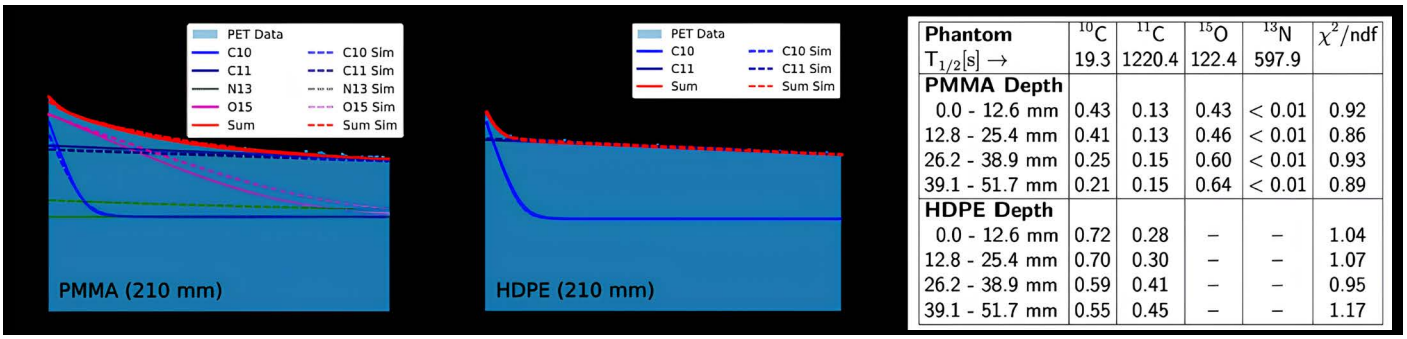

Phantom $T_{1/2}$[s] →	^{10}C 19.3	^{11}C 1220.4	^{15}O 122.4	^{13}N 597.9	χ^2/ndf
PMMA Depth					
0.0 - 12.6 mm	0.43	0.13	0.43	< 0.01	0.92
12.8 - 25.4 mm	0.41	0.13	0.46	< 0.01	0.86
26.2 - 38.9 mm	0.25	0.15	0.60	< 0.01	0.93
39.1 - 51.7 mm	0.21	0.15	0.64	< 0.01	0.89
HDPE Depth					
0.0 - 12.6 mm	0.72	0.28	–	–	1.04
12.8 - 25.4 mm	0.70	0.30	–	–	1.07
26.2 - 38.9 mm	0.59	0.41	–	–	0.95
39.1 - 51.7 mm	0.55	0.45	–	–	1.17

Fig. 8. Post-spill PET coincidence data as a function of time and fits for PMMA and HDPE phantoms. Data are shown as a filled blue histogram, fits are marked by solid lines, while results of Geant4 [51] simulations are shown with dashed lines. The relative abundances of the positron-emitting isotopes produced in these phantoms, determined by these fits, are summarized in the table on the right. We note that our measurements are sensitive to the depth (i.e., the beam energy) at which the isotopes were produced. Figures borrowed from [47].

three projections of images, two of which are displayed in Fig. 9. for one of the PMMA phantoms. Despite a limited range of the field of view, the image clearly shows the penetration of the beam. We note that the PES production does not reflect the Bragg peak

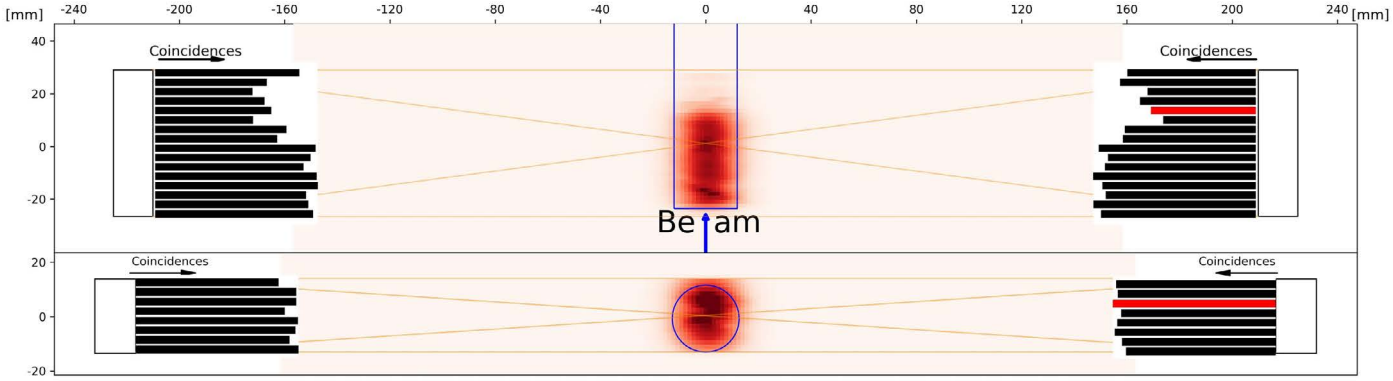

Fig. 9. The coronal (top panel) and axial (bottom panel) views of PET images produced using the CASToR imaging package [50]. The color scale is arbitrary. The cylindrical PMMA 2 phantom is outlined by a rectangle and a circle, and the field of view boundaries are indicated by orange lines. Data were taken in Run 4. For creating these images we used a voxel size of 1.5 × 1.5 × 1.5 mm³, and the results of iteration 5 are shown. The black bars denote the sum of coincidence counts in columns or rows of pixels. Red bars signify a column or row that includes either a dead or noisy pixel, and thus the counts are less reliable. The figure was borrowed from [47].

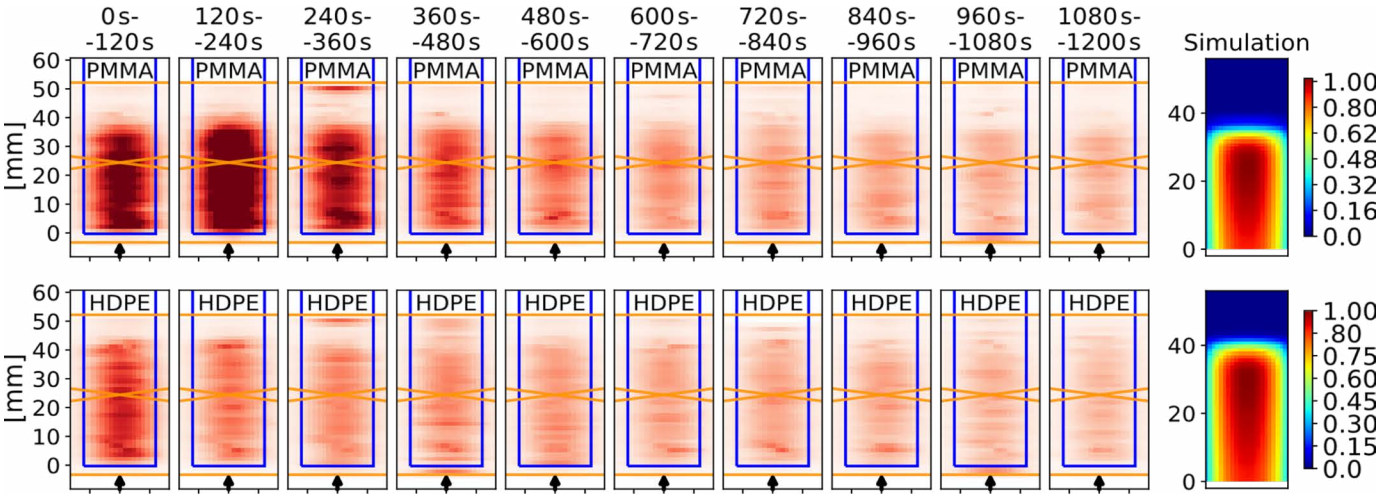

Fig. 10. Frames of coronal PET imaging captured in 120 s-long time periods, marked above each frame for PMMA and HDPE phantoms. The field of view boundaries are indicated by orange lines, while the phantoms are outlined by blue lines. The Geant4 [51] simulated activity produced by the proton beam is shown in the two-dimensional plots on the right. The figures were borrowed from [47].

due to energy-dependent activation cross sections. Our Geant4--based modeling [51] very well reproduces the data, as illustrated in Fig. 8. It is perhaps worth pointing out that the Bragg peak associated with energy loss is significantly smeared in PET signal due to the energy dependence of cross-sections for the production of positron emitters. This is clearly visible in Fig. 9. and 10., and agrees well with our simulations, as discussed in our earlier work, reported in [46] and [47].

OUTLOOK

Our current TPPT scanner can be significantly improved to achieve much higher sensitivity and performance level by constructing it with three independent panels and implementing a double-ended readout of LYSO crystals, as illustrated in Fig. 11. An opening for a proton beam is featured in the central cylindrical section, which can be rotated to assure flexible beam delivery. We have conducted preliminary studies of such an instrument using the Geant4 simulation package and, together with our current tests and experience, are confident that a CTR below 200 ps and a position resolution close to 1 mm can be reached [52].

For a FLASH beam, an addition of a collimator would allow prompt gamma imaging (PGI) through a SPECT technique. Such passive material could be inserted temporarily and removed immediately after the spill. This would allow for capturing the beam image during the short sub-second extraction time. After the removal of the collimator, the PET can follow for a few minutes to provide kinetic imaging and dosimetry, and would be sensitive to washout effects.

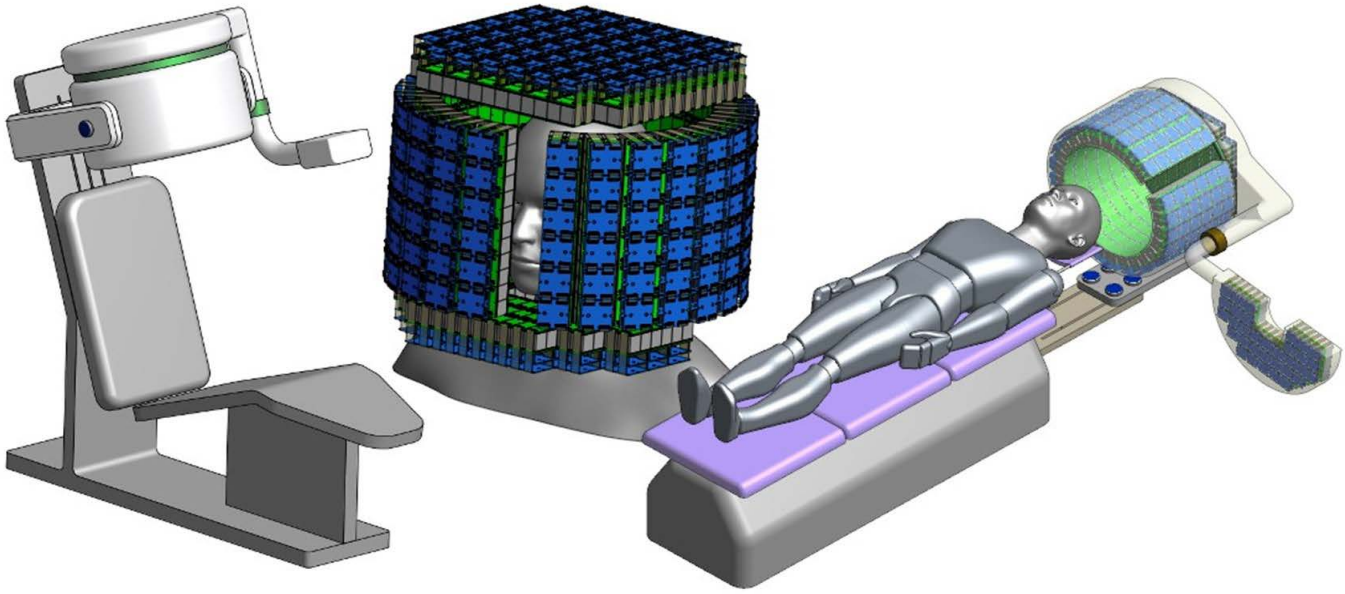

Fig. 11. A three-part PET brain scanner with a cylinder, chin and crown panels that significantly boost the sensitivity of the imager. Additionally, a double-ended readout provides a depth of interaction which further improves coincidence time and position resolutions. An opening slot can be rotated towards the proton beam. The possible implementation of such a scanner is depicted on the left and right.

As argued, there are several aspects of proton therapy that could be improved to introduce image guidance as a routine protocol. We have focused here on the detection options, but this is just one of key elements of this vision that is an integral part of future "personal" medicine.

ACKNOWLEDGEMENTS

We acknowledge support of this work by the University of Texas at Austin and the UT-Portugal program. We thank all members of the TPPT Consortium, supported by the UT Portugal Program at the University of Texas at Austin. The consortium involves researchers from the MD Anderson Proton Center, PETSys Electronics and C2TN in Lisbon, LIP and ICNAS in Coimbra, and the group at the University of Texas at Austin, in particular Marek Proga, John Cesar, Firas Abouzahr, Michael Gajda, Kyle Klein, Alex Kuo, Jingchun Liu, Chris Layden, Will Matava, Aryan Ojha and Akhil Sadam. This work has benefitted from the resources provided by the Texas Advanced Computer Center (TACC) and the high-quality fabrication in the machine shop at the Department of Physics of the University of Texas at Austin. We acknowledge the stimulating and thought-provoking discussions on the above issues with Abass Alavi, Ramin Abolfath, Simon Cherry, Paulo Crespo, Steven Frank, Stan Majewski, Osama Mawlawi, Andrey Morozov, Pawel Moskal, Johan Nuyts, Katia Parodi, Falk Poenisch, Narayan Sahoo, Joao Seco, Ewa Stepien, Stefaan Tavernier and Uwe Titt.

CONFLICT OF INTEREST

Authors have declared no potential conflicts of interest.

REFERENCES

1. www.who.int [Internet]. World Health Organization [cited 2024 July 27]. Available from: https://www.who.int/news/item/0102-2024-global-cancer-burden-growing–amidst-mounting-need-for-services.
2. Wilson RR. Radiological use of fast protons. Radiology 1946 Nov;47: 487-91. doi: https://doi.org/10.1148/47.5.487.
3. ptcog.ch [Internet]. Particle Therapy Co-Operative (PTCOG) Group [cited 2024 July 27]. Available from: https://www.ptcog.ch/index.php/.
4. Parodi K, Enghardt W, Haberer T. In-beam PET measurements of β+ radioactivity induced by proton beams. Phys. Med. Biol. 2002;47:21-36.
5. Enghardt W, Crespo P, Fiedler F, Hinz R, Parodi K, Pawelke J, et al. Charged hadron tumour therapy monitoring by means of PET. NIM-A 2004;525:284-8.
6. Crespo P, Shakirin G, Fiedler F, Enghardt W, Wagner A. Direct time-of-flight for quantitative, real-time in-beam PET: A concept and feasibility study. Phys Med Biol. 2007;52:6795-811.
7. Knopf A, Parodi K, Bortfeld T, Shih HA, Paganetti H. Systematic analysis of biological and physical limitations of proton beam range verification with offline PET/CT scans. Phys. Med. Biol. 2009;54:4477-95. doi: https://doi.org/10.1088/0031-9155/54/14/008.

8. Zhu X, El Fakhri G. Proton therapy verification with PET imaging. Theranostics. 2013 Sep 19;3(10):731-40. doi: https://doi.org/10.7150/thno.5162.

9. Min CH, Zhu X, Winey BA, Grogg K, Testa M, El Fakhri G, et al. Clinical Application of In-Room Positron Emission Tomography for In Vivo Treatment Monitoring in Proton Radiation Therapy. Int J Radiat Oncol Biol Phys. 2013 May 1; 86(1):183-9. doi: https://doi.org/10.1016/j.ijrobp.2012.12.010.

10. Paganetti H, El Fakhri G. Monitoring proton therapy with PET. Br J Radiol 2015;88:20150173. https://doi.org/10.1259/bjr.20150173.

11. Seco J, Clasie B, Partridge M. Review on the characteristics of radiation detectors for dosimetry and imaging. Phys. Med. Biol. 2014;59(20):R303-47. https://doi.org/10.1088/0031-9155/59/20/R303.

12. Seco J, Spadea MF. Imaging in particle therapy: State of the art and future perspective. Acta Oncol. 2015;54(9):1254-8.

13. Shusharina N, Fullerton B, Adams JA, Sharp GC, Chan AW. Impact of aeration change and beam arrangement on the robustness of proton plans. J Appl Clin Med Phys 2019;20(3):14-21. doi: https://doi.org/10.1002/acm2.12503.

14. Grogg K, Zhu X, Shih H, Alpert N, El Fakhri G. Proton Range Verification with PET Imaging in Brain and Head and Neck Cancers. J. Nucl. Med. 2018 May; 59(Supplement 1):658.

15. Durante M, Parodi K. Radioactive Beams in Particle Therapy: Past, Present, and Future. Front Phys. 2020 Aug 28; 8:1-13. doi: https://doi.org/10.3389/fphy.2020.00326.

16. Krishnamoorthy S, Teo B-KK, Zou W, McDonough J, Karp JS, Surti S. A Proof-of-Concept Study of an In-Situ Partial-Ring Time-of-Flight PET Scanner for Proton Beam Verification. IEEE 2021;5:5.

17. Silva F, Campello MPC, Paulo A. Radiolabeled Gold Nanoparticles for Imaging and Therapy of Cancer Materials. Materials. 2021;14(1):4. doi: https://doi.org/10.3390/ma14010004.

18. Favaudon V, Caplier L, Monceau V, Pouzoulet F, Sayarath M, Fouillade C, et al. Ultrahigh Dose-Rate Flash Irradiation Increases the Differential Response Between Normal and Tumor Tissue in Mice. Sci. Trans. Med. 2014;6(245):245ra93. doi: https://doi.org/10.1126/scitranslmed.3008973.

19. Fouillade C, Favaudon V, Vozenin MC, Romeo P-H, Bourhis J, Verrelle P, et al. Hopes of high dose-rate radiotherapy. Bull Cancer 2017;104:380-84.

20. Montay-Gruel P, Petersson K, Jaccard M, Boivin G, Germond J-F, Petit B, et al. Irradiation in a flash: unique sparing of memory in mice after whole brain irradiation with dose rates above 100Gy/s. Radiother Oncol. 2017;124(3):365-69. https://doi.org/10.1016/j.radonc.2017.05.003.

21. Patriarca A, Fouillade C, Auger M, Martin F, Pouzoulet F, Nauraye C, et al. Experimental Set-up for FLASH Proton Irradiation of Small Animals Using a Clinical System. Int J Radiation Oncol Biol Phys 2018;102(3):619-26. doi: https://doi.org/10.1016/j.ijrobp.2018.06.403.

22. Vozenin MC, De Fornel P, Petersson K, Favaudon V, Jaccard M, Germond J-F, et al. The advantage of FLASH radiotherapy confirmed in mini-pig and cat-cancer patients. Clin Cancer Res. 2019 Jan 1;25(1):35-42.

23. Vozenin MC, Hendry JH, Limoli CL. Biological benefits of ultrahigh dose rate FLASH radiotherapy: Sleeping beauty awoken. Clin Oncol (R Coll Radiol). 2019;31(7):407-15.

24. Bourhis J, Montay-Gruel P, Goncalves JP, Bailat C, Petit B, Ollivier J, et al. Clinical translation of FLASH radiotherapy: Why and how? Radiother Oncol. 2019 Oct 8; 139:11-7. doi: https://doi.org/10.1016/j.radonc.2019.04.

25. Montay-Gruel P, Acharya MM, Petersson K, Alikhani L, Yakkala C, Allen BD, et al. Longterm neurocognitive benefits of FLASH radiotherapy driven by reduced reactive oxygen species. Proc Natl Acad Sci USA. 2019 May 28;116(22):10943-51. doi: https://doi.org/10.1073/pnas.

26. Hughes JR, Parsons JL. FLASH Radiotherapy: Current Knowledge and Future Insights Using Proton-Beam Therapy. Int. J. Mol. Sci. 2020;21:6492. doi: https://doi.org/10.3390/ijms21186492.

27. Fouillade C, Curras-Alonso S, Giuranno L, Quelennec E, Heinrich S, Bonnet-Boissinot S, et al. FLASH irradiation spares lung progenitor cells and limits the incidence of radio-induced senescence. Clin Cancer Res. 2020;26(6):1497-1506. https://doi.org/10.1158/1078-0432.CCR-19-1440.

28. Schuler E, Acharya M, Montay-Gruel P, Loo Jr. BW, Vozenin M-C, Maxim PG. Ultra-high dose rate electron beams and the FLASH effect: From preclinical evidence to a new radiotherapy paradigm, Med Phys. 2022;49:2082-95. doi: https://doi.org/10.1002/mp.15442.

29. Lin B, Gao F, Yang Y, Wu D, Zhang Y, Feng G, et al. FLASH Radiotherapy: History and Future. Front. Oncol. 2021;11:644400. doi: https://doi.org/10.3389/fonc.644400.

30. Montay-Gruel P, Acharya MM, Gon P, Jorge C, Petit B, Petridis IG, et al. Hypofractionated FLASH-RT as an Effective Treatment against Glioblastoma that Reduces Neurocognitive Side Effects in Mice. Clin Cancer Res. 2021;27:775-84. doi: https://doi.org/10.1158/1078-0432.CCR-20-0894.

31. Vozenin MC, Bourhis J, Durante M. Towards clinical translation of FLASH radiotherapy. Nat Rev Clin Oncol. 2022;19:791-803. https://doi.org/10.1038/s41571-022-00697-z.

32. Spitz DR, Buettner GR, Petronek MS, St-Aubin JJ, Flynn RT, Waldron TJ, et al. An integrated physico-chemical approach for explaining the differential impact of FLASH versus conventional dose rate irradiation on cancer and normal tissue responses. Radiother Oncol. 2019;139:23-7. doi: https://doi.org/10.1016/j.radonc.2019.03.028.

33. Maxim PG, Keall P, Cai J. FLASH radiotherapy: Newsflash or flash in the pan? Med. Phys. 2019;46:4287-90. doi: https://doi.org/10.1002/mp.13685.

34. Lin B, Gao F, Yang Y, Wu D, Zhang Y, Feng G, et al. FLASH Radiotherapy: History and Future. Front. Oncol. 2021;11:644400. doi: https://doi.org/10.3389/fonc.2021.644400.

35. Favaudon V, Labarbe R, Limoli CL. Model studies of the role of oxygen in the FLASH effect. Med. Phys. 2022;439:2068-81. doi: https://doi.org/10.1002/mp.15129.

36. Leavitt RJ, Almeida A, Grilj V, Montay-Gruel P, Godfroid C, Petit B, et al. Hypoxic tumors are sensitive to FLASH radiotherapy. bioRxiv. 2022;11(27):1-18. doi: https://doi.org/10.1101/2022.11.27.518083.

37. Bogaerts E, Macaeva E, Isebaert S, Haustermans K. Potential Molecular Mechanisms behind the Ultra-High DoseRate "FLASH" Effect, Int. J. Mol. Sci. 2022;23:1-20. doi: https://doi.org/10.3390/ijms232012109.

38. Lin B, Huang D, Gao F, Yang Y, Wu D, Zhang Y, et al. Mechanisms of FLASH effect. Front Oncol. 2022;12:995612. doi: https://doi.org/10.3389/fonc.2022.995612.

39. Wardman P. Radiotherapy Using High-Intensity Pulsed Radiation Beams (FLASH): A Radiation-Chemical Perspective. Radiat. Res. 2020;194:607-17. doi: https://doi.org/10.1667/RADE-19-00016.

40. utaustinportugal.org [Internet]. TOF-PET for Proton Therapy (TPPT) – In-beam Time-of-Flight (TOF) Positron Emission Tomography (PET) for proton radiation therapy, consortium of the University of Texas at Austin (K. Lang, PI), UT Cancer Center (N. Sahoo, PI) and Portugal (V. Varela, PI) [cited 2024 July 27]. Available from: https://utaustinportugal.org/projects/tppt/.

41. mdanderson.org [Internet]. MD Anderson Cancer Center operates in Houston two Proton Therapy Centers. A second center started treating its first patients at the end of 2023 [cited 2024 July 27]. Available from: https://www.mdanderson.org/cmp/proton-therapy.html.

42. Cesar JP, Bugalho R, Caramelo F, Coutinho T, Crespo P, Da Silva JC et al. Time-of-Flight PET for Range Verification in Proton Therapy Treatment. Poster presentation at the 2022 IEEE Nuclear Science Symposium, Medical Imaging Conference and Room Temperature Semiconductor Detector Conference; 2022 Nov 5-12; Milan, Italy.

43. Lang K. Towards high sensitivity and high-resolution PET scanners: Imaging-guided proton therapy and total body imaging, Bio-Algorithms and Med-Systems 2022;18(1):96-106. https://doi.org/10.2478/bioal-2022-0079.

44. petsyselectronics.com [Internet]. PETsys Electronics S.A., Edificio Tecnologia I, 24 e 26 2740-257, Porto Salvo, Oeiras, Portugal [cited 2024 July 27]. Available from: https://www.petsyselectronics.com/web/.

45. hamamatsu.com [Internet]. We used the SiPM model S14161-3050HS-08, manufactured by Hamamatsu Photonics K. K., Hamamatsu City, Japan, and Bridgewater, NJ 08807-0910, USA [cited 2024 July 27]. Available from: https://www.hamamatsu.com.

46. Abouzahr F, Cesar JP, Crespo P, Gajda MJ, Hu Z, Kaye W, et al. The first PET glimpse of a proton FLASH beam, Phys. Med. Biol. 2023;68:125001. doi: https://doi.org/10.1088/1361-6560/acd29e.

47. Abouzahr F, Cesar JP, Crespo P, Gajda MJ, Hu Z, Kaye W, et al. The first probe of a FLASH proton beam by PET. Phys. Med. Biol. 2023;68:235004. doi: https://doi.org/10.1088/1361-6560/ad0901.

48. Titt U, Yang M, Wang X, Iga K, Fredette N, Schueler E, et al. Design and validation of a synchrotron proton beam line for FLASH radiotherapy preclinical research experiments. Med Phys. 2021;49(1):1-13 doi: https://doi.org/10.1002/mp.15370.

49. Bass SD, Mariazzi S, Moskal P, Stepien E. Colloquium: Positronium physics and biomedical applications. Rev. Mod. Phys. 2023;95;021002.

50. Merlin T, Stute S, Benoit D, Bert J, Carlier T, Comtat C, et al. CASToR: A generic data organization and processing code framework for multi-modal and multi-dimensional tomographic reconstruction. Phys. Med. Biol. 2018;63:185005. doi: https://doi.org/10.1088/1361-6560/aadac1.

51. Agostinelli S, Allison J, Amako K, Apostolakis J, Araujo H, Arce P, et al. Geant4 – A Simulation Toolkit. Nucl. Instrum. Meth. A 2003;506:250-303.

52. Layden C, Klein K, Matava W, Sadam A, Abouzahr F, Proga M, et al. Design and modeling of a high-resolution and high-sensitivity PET brain scanner with double-ended readout, Biomed. Phys. Eng. Express 2022;8:025011.